Nova Science Publishers, Inc.
Hauppauge, New York
Journal of Nature Science and Sustainable Technology, Volume 1, Issue 4, 2007

A NOVEL MEMORY BASED STRESS-STRAIN MODEL FOR RESERVOIR CHARACTERIZATION

M. Enamul Hossain
S. Hossein Mousavizadegan
Chefi Ketata
M. Rafiqul Islam
Department of Civil & Resource Engineering, Dalhousie University
Sexton Campus, 1360 Barrington Street, Halifax, NS B3J 2X4, Canada

ABSTRACTS

The fluid memory is the most important yet most neglected feature in considering fluid flow models, since it represents the history of the fluid and how it will behave in the future. This paper introduces a stress-strain model where all the probable properties have been incorporated with viscous stresses. The derived mathematical model introduces the effect of temperature, the surface tension, pressure variations and the influence of fluid memory on the stress-strain relationship. The part of the stress-strain formulation related to the memory is taken into account and we obtain the variation of it with time and distance for different values of α. The notation α is shown the effect of memory and varied $0 \leq \alpha < 1$. The zero value shows no memory effect while the unity values of α shows the most extreme case of the effect of memory. The fluid memory effects as a function of space and time are obtained for the fluid in a sample oil reservoir. The dependency of fluid memory is considered to identify its influence on time. As pressure is also a function of space, the memory effects are shown in space with pressure gradient change. The computation indicates that the effect of memory cause a nonlinear and chaotic behavior for stress-strain relation. This model can be used in reservoir simulation and rheological study, well test analysis, and surfactant and foam selection for enhanced oil recovery.

INTRODUCTION

The impact of viscosity in reservoir is directly related to oil production. The mobility of the crude oil increases by lowering the fluid viscosity and consequently, it enhances the oil recovery. A fluid can not resist the shear forces and starts to move and deform regardless of the amount of the shear forces. Its shape will change continuously as long as the force is applied. The relationship between the rate of strain and the shear stress specifies the type of fluid from viscosity points of view. Typically, viscous stresses within a fluid tend to stabilize and organize the flow, whereas excessive fluid inertia tends to disrupt organized flow leading to chaotic turbulent behavior.

A Novel Memory Based Stress-Strain Model for Reservoir Characterization

The Newton law of viscosity is based on a linear relationship between the viscous stress and the rate of strain. A fluid that satisfies this law is called the Newtonian fluid. The coefficient of proportionality is known as the viscosity that depends only on temperature and pressure and also the chemical composition of the fluid if the fluid is not a pure substance. For a Newtonian fluid, the viscosity does not depend on the forces acting upon it at all shear strain rate. Water, some light-hydrocarbon oils, air and other gases are Newtonian fluids. In contrast, a fluid that has not a well-defined viscosity is called the non-Newtonian fluid. The viscosity of such a fluid changes with the applied forces and strain rates. The Newton model considers the parallel plate concept in fluid flow. The roles of surface tension or interfacial tension on the viscosity of a fluid, and memory of a fluid have been ignored in this model.

In the reservoir, the structure of the formation media is important to consider because the dependency of pore size and microstructure influences the oil flow. Pressure and temperature are the influential factors in flow criteria in porous media where pressure is the most dominant parameter (Hossain et al. 2006). The strain rate in porous media is affected by the velocity of the formation fluid that depends on the pressure variation and in some respect on temperature. This may leads to a non-Newtonian behavior of the crude oil. However, the deviation of the crude oil behavior from a Newtonian fluid is dependent on the formation temperature and also the composition of the crude oil. Crude oil is the outcome of living things which existed millions of years ago like fossils in nature. The American Petroleum Institute (API) defines crude oil as “a substance, generally liquid, occurring naturally in the earth and composed mainly of mixtures of chemical compounds of carbon and hydrogen with or without other nonmetallic elements such as sulfur, oxygen, and nitrogen”. It is a complicated mixture of hydrocarbons, with a varying composition depending on its source and pathway. It contains different functional groups, such as paraffins, aromatics, napthenes, resins, and asphaltenes, which may cause dramatic change in the rheological behavior due to the variation of temperature and pressure.

Surface tension is one of the most important fluid properties that govern the fluid flow. Marangoni effect for the fluid layer is considered to represent the effect of surface tension. The Marangoni effect is a phenomenon of interfacial turbulence provoked by surface tension gradients that might be induced by gradients in temperature, concentration and surface charge through the interface (D’Aubeterre et al., 2005). These researchers have given an extensive review of Marangoni effect in heat and mass transfer process. This effect efficiently enhances the rate of mass transfer across the interface. The importance of the Marangoni convection on heat and mass transfer processes in porous media is known by the researchers because of the development of the instabilities at the interface during these two processes. So, the understanding of the behavior of Marangoni effect is very important from both theoretical and practical point of view. This effect is also important in many separation processes such as distillation, absorption and extraction because the convective flows due to the Marangoni effect and other phenomena can lead to increase mass transfer and interfacial turbulence.

Lyford et al. (1998a) concluded that the use of surfactant such as aliphatic alcohol increases the oil recovery in porous media which is due to Marangoni effect. This effect makes oscillations in the droplets trapped in the pores. The cause of oil recovery is the Marangoni interfacial turbulence induced by concentration gradients of solute established by the mass transfer between the trapped droplets and the continuous phase inside the porous

media. As a result, Lyford et al. (1998b) proposed that these effects must be characterized by the Marangoni number (M_a), which relates the surface tension gradient with concentration; instead of by the Capillary number (Ca). Moreover, Bragard and Velarde (1998) argued that it is important to understand the instabilities of droplets and bubbles induced by the Marangoni effect. He established that the Marangoni effect is the physicochemical motor which transforms energy in flow and is based on the presence of temperature and concentration gradients, the fluid viscosity and diffusivity.

The stress-strain relation should be time dependent and consider the effect of pathway and fluid memory. In nature, groundwater, oil, gas and other fluids behave according to the pathway traveled by every particle. The conventional approach in reservoir engineering has focused on the permeability of solid and semi-solid structures encountered by the flow of the fluid. What it doesn't do is follow these pathways. Fluid memory is an approach to factor this back in by switching the frame of reference from the external observation of flow to that of matter molecules within the flow. The literature to date has yet to conceptualize fluid memory in a comprehensive way. The particularity and uniqueness of memory is that its definition varies with different combinations of any given fluid and its particular medium which has posed the greatest difficulty. Memory itself is a function of all possible properties of the given fluid and its medium over time. Fluid materials have some common properties but some have special properties that are remarkable in the behavior when some forces are applied on them. In some nonlinear, incompressible and viscous fluids, they possess some peculiar characteristics that lead to think about something else on their properties especially for viscous fluids. The phenomenon that describes these special characteristics is remarked as memory in fluid. There are very limited studies in the literature that describe this phenomenon clearly. However, an extensive review is done here which leads to introduce the notion of memory of fluids.

Jossi et al. (1962) developed a correlation to calculate the viscosity of the pure fluid in terms of the pressure, temperature and properties of the chemical species. Their correlation is suitable to reduced density in the range 0.1 and 3.0. This correlation is valid for the viscosity of nonpolar substances. Because of the inadequacy of current theories in accounting for memory, some authors also developed non-local flow theories (e.g. Hu and Cushman, 1994), using general principles of statistical physics under appropriate limiting conditions from which the classical Darcy's law is derived for saturated flow. Starov and Zhdanov (2001) studied the effective properties of porous media. They correlated viscosity and a resistance coefficient (1/permeability) using Brinkman's equations. They also established the relation between the porosity and viscosity. Abel et al. (2002) studied the boundary layer flow and heat transfer of a visco-elastic fluid immersed in a porous medium over a non-isothermal stretching sheet. They concluded that the fluid viscosity is a function of temperature. Their case study involved to get the effect of fluid viscosity, permeability parameter and visco-elastic parameter for various situations. Their finding is that the effect of fluid viscosity parameter decreases the wall temperature profile significantly when flow is through a porous medium. Further, the effect of permeability parameter decreases the skin friction on the sheet. Brenner (2005) reviewed the Newton's law of viscosity. He found the role of the deviatoric stress tensor in the Navier–Stokes equation for the case of compressible fluids, both gaseous

and liquid. He proposed the replacement of velocity gradient term, fluid's mass-based velocity in Newton's law of viscosity by the fluid's volume velocity (volume flux density). He has shown how stress tensors are related with density of a fluid.

Ciarletta et al. (1989) concerned with variational questions about the linearized evolution equations for an incompressible fluid whose viscosity exhibits a fading memory of the past motions. Nibbi (1994) had determined the expressions of some free energies related to viscous fluids with memory. He also considered the quasi-static problem connected with a viscous fluid with memory. Broszeit (1997) dealt with the numerical simulation of circulating steady isothermal flow for liquids with memory. Caputo (1999) investigated in some geothermal areas where the fluids may precipitate minerals in the pores of the medium, leading to diminished sizes. He modified the Darcy's law by introducing a memory formalism represented by a derivative of fractional order simulating the effect of a decrease of the permeability with time. He pointed out some influential parameters that may govern the pore size. The change of pore size influences permeability changes. He also pointed out that permeability diminishes with time and the effect of fluid pressure at the boundary of the pore network on the fluid flow through the medium is delayed and that the flow occurs as if the medium has a memory. Eringen (1999) developed nonlocal theory of memory dependent micropolar fluids with orientational effects. Orientational and nonlocal effects near the walls change viscosity drastically if polymeric fluids squeezed in microscopic sizes. Li et al. (2001) investigated air bubble in non-Newtonian fluids. They identified two aspects for the first time as central to interactions and coalescence: (i) the stress creation by the passage of bubbles, and (ii) their relaxation due to the fluid's memory. Their results show complex nonlinear dynamics, from periodic phenomena to deterministic chaos. Recently, Hossain and Islam (2006) have presented an extensive review of literatures on this memory issue. They critically reviewed almost all the existing models and showed theirs limitations. They also showed how memory of a fluid and media play a great role on stress-strain relation.

The effects of all parameters are considered to obtain a comprehensive model for the stress-strain rate relation for crude oil behavior in the reservoir formation. The effects of surface tension, temperature, pressure, and the fluid memory are taken into account. The effect of surface tension is considered through the application of Marangoni number (M_a) that explains the role of surface tension. The effect of memory is explained with a dominant variable, the fractional order of differentiation (α), and a constant, ratio of the pseudo-permeability of the medium with memory to fluid viscosity (η). The value of α is changed to identify the effects of memory of the fluid. The results are presented in a graphical form to demonstrate the effect of fluid memory. The results show that the effect of memory causes a nonlinear relationship between memory part of the model and time and space. This nonlinearity is due to the dependency of pressure to the fluid velocity. However, there also exists a chaotic and unpredictable effect on the variation of the fractional order of differentiation.

THEORETICAL DEVELOPMENT

If a tangential force *F* is acting on the upper surface of a fluid element, ABCDEFGH, in a porous media, AIJKLMNO, in the *x*-direction, the fluid element will deform as shown in Figure 1. The deformation is caused by shearing forces which act tangentially to a surface, CDEF.

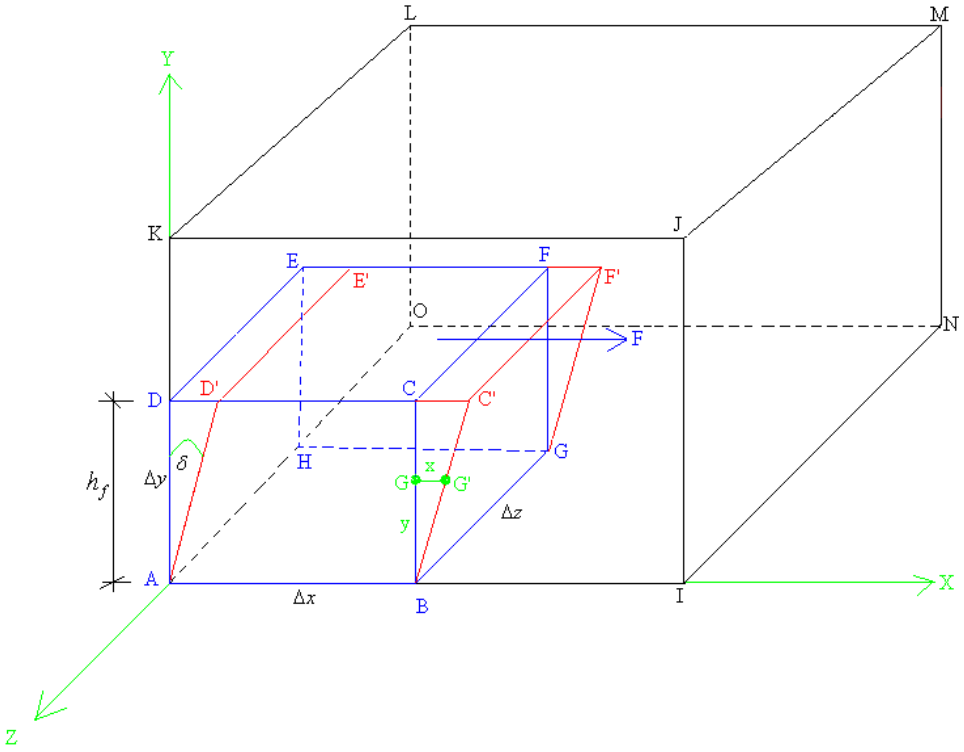

Figure 1 Fluid element under a shear force

The shear stress and the rate of deformation are normally expressed by the Newton's law of viscosity which can be written mathematically as;

$$\tau = \mu \frac{du_x}{dy} \tag{1}$$

Now for at any temperature *T* and in the *x*-direction, Newton's law of viscosity can be written down into the form;

$$\tau_T = \mu_T \frac{du_x}{dy} \tag{2}$$

However, this relation is not valid in many cases such as crude oil behavior in porous media.

Effect of temperature on Fluids

There is some molecular interchange between adjacent layers in liquids but as the molecules are so much closer than in gasses the cohesive forces hold the molecules in place much more rigidly. This cohesion plays an important role in the viscosity of liquids. Increasing the temperature of a fluid reduces the cohesive forces and increases the molecular interchange. Reducing cohesive forces reduces shear stress, while increasing molecular interchange increases shear stress. Because of this complex interrelation the effect of temperature on viscosity has been described by various models depending on industrial applications (Recondo et al., 2005). In this study, the Arrhenius model is used to describe the viscosity dependence on temperature (Avramov, 2005; Recondo et al., 2005; Zuritz et al., 2005; Haminiuk et al., 2006; Gan et al., 2006)

$$\mu_T = \mu_0 e^{\left(\frac{E}{RT}\right)} \tag{3}$$

Putting the value of μ_T of equation (3) into equation (2) gives;

$$\tau_T = \left[\mu_0 \, e^{\left(\frac{E}{RT}\right)}\right] \frac{du_x}{dy} \tag{4}$$

High pressure can also change the viscosity of a liquid. As pressure increases the relative movement of molecules requires more energy. Hence viscosity increases, which influences the stress-strain relationship. This effect has been ignored by former researchers.

Effect of Surface Tension and pressure on Fluids

However, in order to obtain more representative values of the Marangoni effect, it is necessary to isolate the effect from other phenomena such as the natural convection produce by gravity and the presence of surfactants or other agents that can disturb the concentration gradients. Therefore, in the present study, the initial temperature has been considered as 298°K at the plan of ABGH and a certain temperature, *T* °K at the plan of CDEF along the *y*-direction (see Figure 1). If the changes in surface tension are produced by temperature gradients, the Marangoni number is expressed as follows (Das and Bhattacharjee, 1999; Haferl and Poulikakos, 2003; Kozak et al., 2004; D'Aubeterre et al., 2005):

$$M_a = \left|\frac{\partial \sigma}{\partial T}\right| \frac{h_f \Delta T}{\alpha_D \mu_0} \tag{5}$$

Putting the value of μ_0 into Equation (4) and gives:

$$\tau_T = \left[\left(\frac{\partial \sigma}{\partial T} \frac{h_f \Delta T}{\alpha_D M_a} \right) \times e^{\left(\frac{E}{RT} \right)} \right] \frac{du_x}{dy} \tag{6}$$

If we consider molecularly thin film hydrodynamic fluid behavior in rock matrix, the influence of the fluid discontinuity across the fluid film thickness on the total fluid mass flow through the contact is determined by an operational parameter, *K*, which is defined as (Zhang and Lu, 2005):

$$K = \frac{\partial p / \partial x \times h_f^2}{6\mu_0 (1-\zeta)(u_a - u_b)}$$

If we consider no slip condition and there is no lower contact surface velocity, the above equation can be written as:

$$K = \frac{\partial p / \partial x \times h_f^2}{6\mu_0 u_x}$$

$$h_f^2 = \frac{6K\mu_0 u_x}{\partial p / \partial x}$$

It should be mentioned here that in the present molecularly thin film hydrodynamic flow, when the value of the operational parameter K is high, i.e., over 0.1, the influence of the fluid discontinuity across the fluid film thickness on the total fluid mass flow through the contact is significant. When the value of the operational parameter K is low, i.e., close to zero, this influence is negligible (Zhang and Lu, 2005). Putting the value of film thickness, h_f into Equation (6) becomes:

$$\tau_T = \left(\frac{\partial \sigma}{\partial T} \frac{\Delta T}{\alpha_D M_a} \right) \times \left(\frac{6K\mu_0 u_x}{\partial p / \partial x} \right)^{1/2} \times e^{\left(\frac{E}{RT} \right)} \frac{du_x}{dy} \tag{7}$$

Effect of Fluid Memory on Viscosity

To incorporate the fluid memory criterion with stress relation, the mass flow rate in porous media can be represented by the following equation (Caputo, 1999). If the direction of flow is in *x*-direction, the equation can be written as:

$$q_x = -\eta \rho_0 \left[\frac{\partial^\alpha}{\partial t^\alpha} (\partial p / \partial x) \right] \tag{8}$$

where

A Novel Memory Based Stress-Strain Model for Reservoir Characterization

$$\partial^{\alpha}\{p(x,t)\}/\partial t^{\alpha} = [1/\Gamma(1-\alpha)]\int_0^t (t-\xi)^{-\alpha}[\partial p(x,\xi)/\partial \xi]\,d\xi \quad \text{with } 0 \le \alpha < 1$$

Equation (8) can be written as:

$$u_x = -\eta\left[\frac{\partial^{\alpha}}{\partial t^{\alpha}}(\partial p/\partial x)\right]$$

where, u_x is the fluid velocity in porous media. Putting the value of u_x onto Equation (7) yields

$$\tau_T = \left(\frac{\partial \sigma}{\partial T}\frac{\Delta T}{\alpha_D M_a}\right)\times\left\{-\frac{6K\mu_0\,\eta\left[\frac{\partial^{\alpha}}{\partial t^{\alpha}}(\partial p/\partial x)\right]}{\partial p/\partial x}\right\}^{1/2} \times e^{\left(\frac{E}{RT}\right)}\frac{du_x}{dy} \qquad (9)$$

where

$$\partial^{\alpha}\{\partial p(x,t)/\partial x\}/\partial t^{\alpha} = [1/\Gamma(1-\alpha)]\int_0^t (t-\xi)^{-\alpha}\left[\partial\left(\frac{\partial p}{\partial x}\right)\Big/\partial \xi\right]d\xi$$

or,

$$\partial^{\alpha}\{\partial p(x,t)/\partial x\}/\partial t^{\alpha} = [1/\Gamma(1-\alpha)]\int_0^t (t-\xi)^{-\alpha}\left[\frac{\partial^2 p}{\partial \xi \partial x}\right]d\xi$$

As a result, Equation (9) becomes

$$\tau_T = \left\{-\frac{6K\mu_0\eta[1/\Gamma(1-\alpha)]\int_0^t (t-\xi)^{-\alpha}\left[\frac{\partial^2 p}{\partial \xi \partial x}\right]d\xi}{\partial p/\partial x}\right\}^{1/2} \times\left(\frac{\partial \sigma}{\partial T}\frac{\Delta T}{\alpha_D M_a}\right)\times e^{\left(\frac{E}{RT}\right)}\frac{du_x}{dy}$$

$$\tau_T = \left(\frac{\partial \sigma}{\partial T}\frac{\Delta T}{\alpha_D M_a}\right)\times\left\{-\frac{6K\mu_0\eta\int_0^t (t-\xi)^{-\alpha}\left[\frac{\partial^2 p}{\partial \xi \partial x}\right]d\xi}{\Gamma(1-\alpha)\frac{\partial p}{\partial x}}\right\}^{0.5} \times e^{\left(\frac{E}{RT}\right)}\frac{du_x}{dy}$$

$$\tau_T = (-1)^{0.5} \times \left(\frac{\partial \sigma}{\partial T} \frac{\Delta T}{\alpha_D M_a} \right) \times \left\{ \frac{\int_0^t (t-\xi)^{-\alpha} \left[\frac{\partial^2 p}{\partial \xi \partial x} \right] d\xi}{\Gamma(1-\alpha)} \right\}^{0.5} \times \left(\frac{6K\mu_0 \eta}{\frac{\partial p}{\partial x}} \right)^{0.5} \times e^{\left(\frac{E}{RT} \right)} \frac{du_x}{dy} \quad (10)$$

The above mathematical model provides the effects of the fluid and formation properties in one dimensional fluid flow and this model may be extended to a more general case of 3-Dimensional flow for a heterogeneous and anisotropic formation. However, this may be concluded that, although other causes such as heterogeneity, anisotropy, and inelasticity of the matrix may be invoked to interpret certain phenomena, the memory mechanism could help in interpreting part of the phenomenology. It should be mentioned here that the first part of the Equation (10) is the effects of surface tension, second part is the effects of fluid memory with time and the pressure gradient, the third part is the effects of pressure, viscosity, pseudo-permeability, the fourth part is the effects of temperature on stress-strain equation and the fifth part is the velocity gradient in *y*-direction which is called rate of velocity change i.e. rate of shear strain. The second part is in a form of convolution integral that shows the effect of the fluid memory during the flow process. This integral has two variable functions of $(t-\xi)^{-\alpha}$ and $\partial^2 p / \partial \xi \partial x$ where the first one is a continuous changing function and second one is a fixed function. This means that $(t-\xi)^{-\alpha}$ is an overlapping function on the other function, $\partial^2 p / \partial \xi \partial x$, in the mathematical point of view. These two functions depend on the space, time, pressure, and a dummy variable.

CASE STUDY

The results of the stress-strain rate based on the model presented in Equation (10) can be obtained by solving this equation. In this paper, we focused on the second part of the formulation that is related to the effect of fluid memory and finding a numerical description for a sample reservoir.

A reservoir of length (L = 5000.0 m), width ($W = 100.0$ m) and height, (H = 50.0 m) have been considered. The porosity and permeability of the reservoir are 30% and 30md, respectively. The reservoir is completely sealed and produces at a constant rate where the initial pressure is p_i = 27579028 pa (4000 psia). The fluid is assumed to be API 28.8 gravity crude oil with the properties $c = 1.2473 \times 10^{-9}\ 1/pa$, $\mu_0 = 87.4 \times 10^{-3}$ *Pa-s* at 298°K. The initial production rate is $q_i = 8.4 \times 10^{-9}$ m^3/sec and the initial fluid velocity in the formation is $u_i = 1.217 \times 10^{-5}$ m/sec. The fractional order of

differentiation, $\alpha = 0.2 - 0.8$, $\Delta x = 100.0$ m; and $\Delta t = 7.2 \times 10^4$ sec have also been considered. The computations are carried out for $Time = 10,\ 50$ and 100 months and at a distance of $x = 1500,\ 3000$ and 4500 meters from the wellbore. In solving this convolution integral with memory, trapezoidal method is used. All computation is carried out by Matlab 6.5.

Pressure distribution

To solve the convolution integral in Equation (10), it is necessary to obtain the pressure distribution along the reservoir. The pressure distribution is assumed to be modeled through the diffusivity equation in porous media. This equation has been derived by combining the continuity equation with the Darcy's law as the momentum equation.

$$\frac{\partial^2 p}{\partial x^2} = \frac{\phi \mu_0 c}{k} \frac{\partial p}{\partial t} \tag{11}$$

To solve this equation, the following dimensionless parameters are considered.

$$x^* = \frac{x}{L},\ t^* = \frac{u_i t}{L},\ p^* = \frac{p}{p_i}, \text{ and } q^* = \frac{q}{q_i} \tag{12}$$

Using the dimensional parameters from Equation (12), Equation (11) can be written in dimensionless form as

$$\frac{\partial^2 p^*}{\partial x^{*2}} = \frac{L \phi \mu_0 c u_i}{k} \frac{\partial p^*}{\partial t^*} \tag{13}$$

It is defined that $a_2 = \frac{L \phi \mu_0 c u_i}{k}$ in Equation (13) and therefore, it may be written that

$$\frac{\partial p^*}{\partial t^*} = \frac{1}{a_2} \frac{\partial^2 p^*}{\partial x^{*2}}. \tag{14}$$

The initial condition is $p^*(x^*, 0) = 1$. The boundary condition is $\partial p^*(1, t^*) / \partial x^* = 0$ at the outer boundary and the boundary condition at the wellbore is $q^* = c_1 \partial p^* / \partial x^*$, where $c_1 = -kA_{yz} p_i / \mu L q_i$. The implicit scheme is applied to solve Equation (14) with finite difference method. The discretized form of Equation (14) is

$$p_i^{*(n+1)} = p_i^{*n} + \frac{1}{a_2}\frac{\Delta t^*}{\left(\Delta x^*\right)^2}\left[p_{(i+1)}^{*n} - 2\,p_i^{*n} + p_{(i-1)}^{*n}\right] \qquad (15)$$

where Δt^* is the time step and Δx^* is the grid size. According to James et al. (1993), the solution of Equation (15) will be stable and nonoscillatory for boundary conditions that remain constant with time if $\Delta t^* \big/ a_2\left(\Delta x^*\right)^2 \le 0.25$ and will be stable only if $0.25 < \Delta t^* \big/ a_2\left(\Delta x^*\right)^2 \le 0.50$. Equation (15) can be written as

$$p_i^{*(n+1)} = \left(1 - 2a_1\right)p_i^{*n} + a_1\left(p_{(i+1)}^{*n} + p_{(i-1)}^{*n}\right) \qquad (16)$$

where, $h = \Delta t^* \big/ \left(\Delta x^*\right)^2$ and $a_1 = h \big/ a_2$. This equation can be solved using the specified initial and boundary conditions.

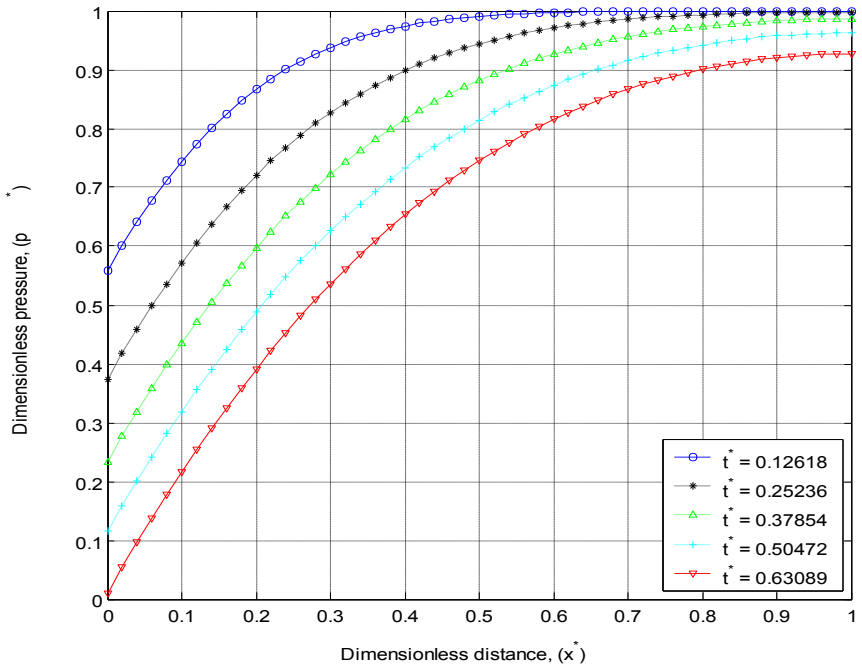

Figure 2 Dimensionless pressure variation with dimensionless distance

Figure 2 shows the dimensionless pressure variation with dimensionless distance for different dimensionless time. The pressure is increasing with distance from the wellbore towards the outer boundary. In the boundary, the pressure remains almost constant. As time passes, the pressure starts to decrease more rapidly towards the outer boundary and it goes down more comparing with previous time step.

A Novel Memory Based Stress-Strain Model for Reservoir Characterization

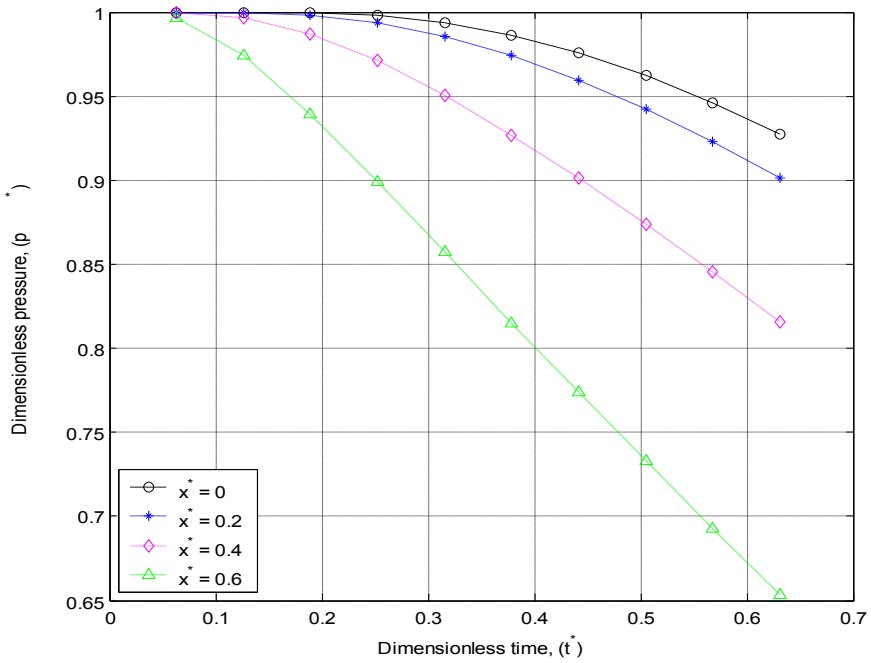

Figure 3 Dimensionless pressure variation with dimensionless time for different dimensionless distance

Figure 3 shows the dimensionless pressure variation with dimensionless time for different dimensionless distance. The trend of pressure is decreasing with time towards the boundary of the reservoir. The pressure decline is sharper and more rapid with time from wellbore towards the boundary. This indicates that at the initial stage of the production, the pressure decline is lower than the one encountered in the next production level by the boundary of the reservoir.

Figure 4(a) represents the pressure gradient as a function of time for different distances from wellbore towards the outer boundary of the reservoir. Initially, the pressure gradient is less affected around the wellbore. It rises with time gradually around the wellbore and the slope of the gradient is positive. At the boundary, the pressure gradient is constant. At the wellbore, it approaches zero.

Figure 4(b) shows the pressure gradient in *x*-direction as a function of distance from the wellbore towards the outer boundary of the reservoir for different time steps. Initially the pressure gradient drop is rapid and higher around the wellbore. It drops very fast and sharply from wellbore toward reservoir boundary. As time passes, pressure gradient decline goes slower with distance and become more stable. This indicates that for larger and larger time, the pressure derivative goes towards its stable condition.

Figure 4(c) displays the pressure gradient change over time in the x direction ($\partial^2 p/\partial x\,\partial t$) as a function of time for different distance values. The $\partial^2 p/\partial x\,\partial t$ change is not very recognizable around the wellbore side throughout the life span of a reservoir. However, this change becomes more important, reportable, and influential at the initial stage of the reservoir production in the position of its outer boundary region and its surroundings.

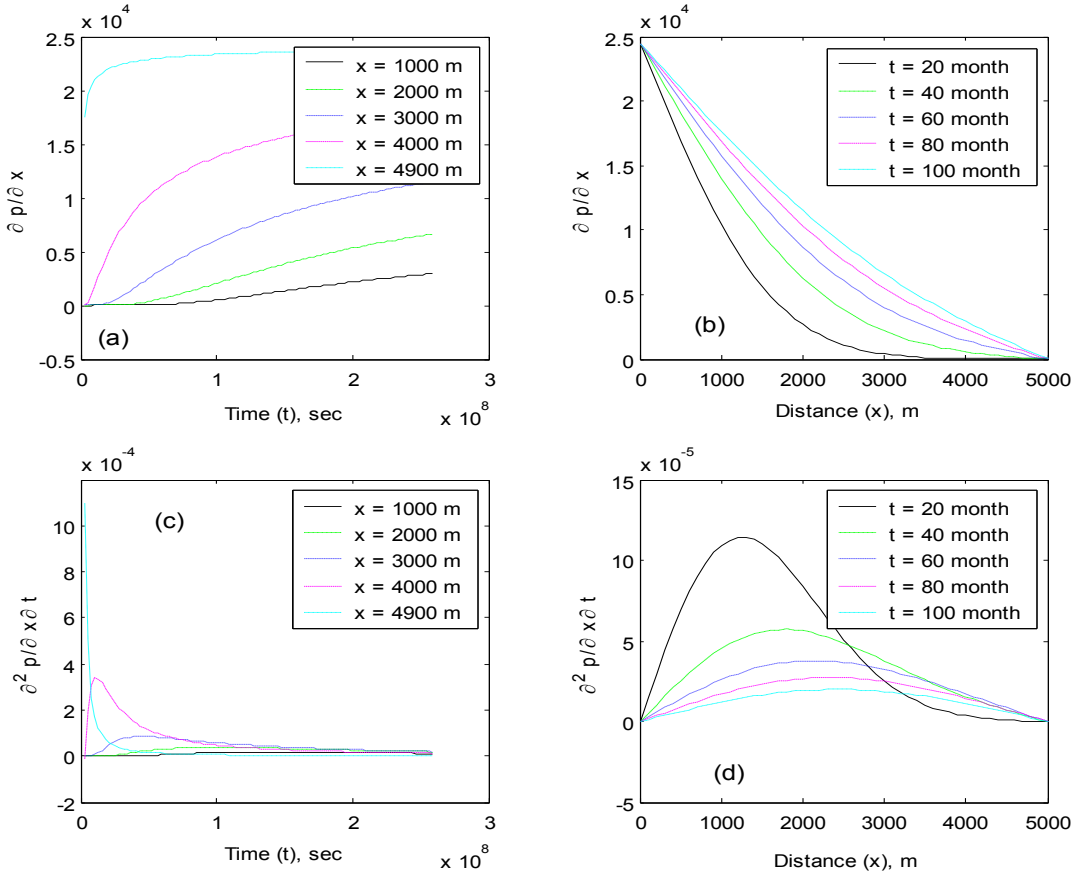

Figure 4 Pressure gradient in x direction for different time steps and distance from the wellbore

Figure 4(d) displays the pressure gradient change over time in the x direction ($\partial^2 p/\partial x\,\partial t$) as a function of distance for different time steps. Initially, $\partial^2 p/\partial x\,\partial t$ change is very sharp and affective especially around the wellbore. It turns out to reduce also very quickly with distance towards the outer boundary. However, this pattern changes gradually with time. These variations throughout the reservoir become closer for longer time. The direction of slope change (i.e. from positive to negative) shifts its position from wellbore side towards the outer boundary with time.

Figure 5(a) shows the pressure change over time as a function of time for different distances from the wellbore. Throughout the reservoir life, the pressure change over time is not very affective especially around the wellbore. However, this pattern changes gradually towards the outer boundary of the reservoir with time. The direction of the curve slope and shape change is very fast during the initial stage throughout the reservoir. These variations throughout the reservoir become closer for longer time period.

Figure 5(b) shows the pressure change over time as a function of distance from the wellbore towards the boundary of the reservoir for different time steps. The direction pattern of the pressure change over time is characterized by an *S*-shape. At the initial stage of production, the shape and the direction of the pressure change over time illustrate rapid and sharp variation around the wellbore. However, this pattern changes gradually with time and advances to become constant towards the outer boundary of the reservoir. The slope of the curve decreases gradually comparing with previous time step. This advancement indicates that the pressure change over time reaches its steady state for larger and larger time. Therefore, the reservoir behavior is more stable in the long term than in the short term.

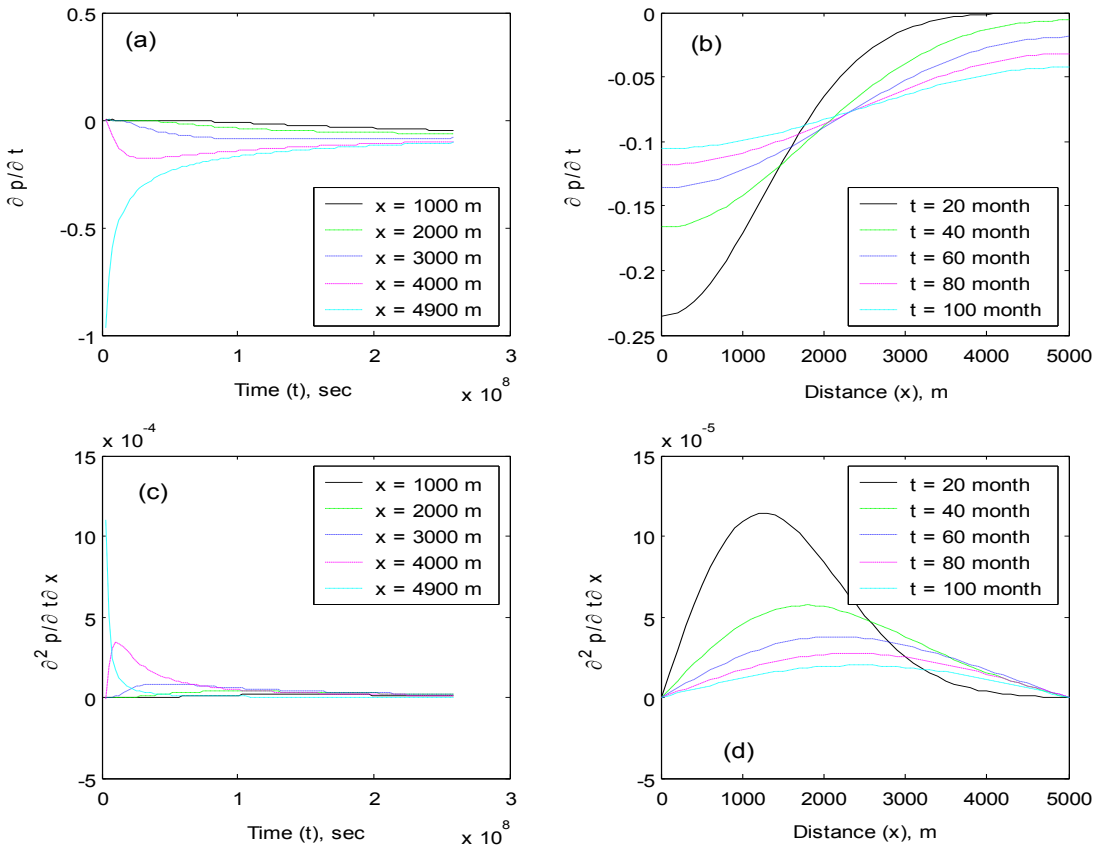

Figure 5 Pressure change over time and distance in the *x* direction for different time steps and distance from the wellbore

Figure 5(c) displays the pressure gradient change over time in the x direction ($\partial^2 p/\partial t\,\partial x$) as a function of time for different distance values. Figure 5(d) displays the pressure gradient change over time in the x direction ($\partial^2 p/\partial t\,\partial x$) as a function of distance for different time steps. Both figures are same as figures 4(c) and 4(d).

RESULTS AND DISCUSSION

The stress-strain relationship is given in Equation 10. The effect of the memory of the fluid flow is distributed in the second and third parts of it as we describe it already. Here, we have the fluid memory parameters with pressure distribution in space and time. The ratio of the pseudopermeability of the medium with memory to fluid viscosity (η) is considered as a constant. So, the effect of memory due to this parameter is constant with pressure distribution in the formation. It does not change with space and time. The most influential parameter for the effect of memory is the fractional order of differentiation (α) which is related to pressure distribution, space and time. This is in the second part of Equation 10 and identified by I_{mi} as;

$$I_{mi} = \left\{ \frac{\int_0^t (t-\xi)^{-\alpha} \left[\partial^2 p/\partial \xi\, \partial x\right] d\xi}{\Gamma(1-\alpha)} \right\}^{0.5} \tag{11}$$

In Equation 11, the fractional derivative α exists on both numerator and denominator. It ranges from 0 to 1. The denominator, $[\Gamma(1-\alpha)]^{0.5}$, varies as a function of α as presented in Fig. 6. It changes as follows: $1 \le [\Gamma(1-\alpha)]^{0.5} < \infty$.

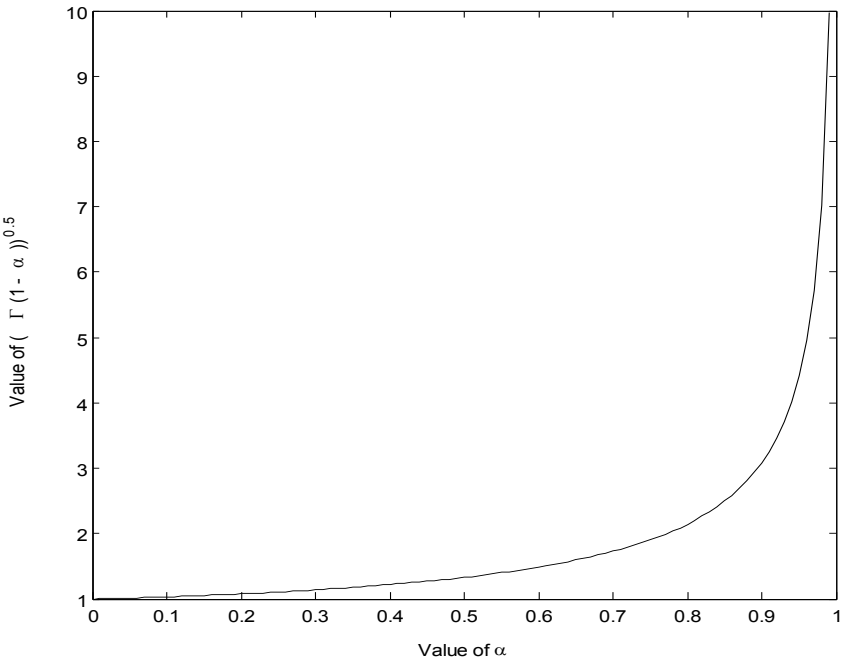

Figure 6 Variation of Gamma part of memory of Equation (10) over α

DEPENDENCE ON TIME

At different distance from the wellbore

The effect of the memory is given in Equation 11 and identifies By I_{mi}. This is a function of time and space. We studied the variation of it with respect to time and space for the sample reservoir that we explained already. Duration of 100 months is taken into account to find the effect of value of memory at different distances from the wellbore.

Figure 7 shows the change of I_{mi} for different α values for duration of 100 months at a distance of 1500 m from the wellbore. The value of I_{mi} is varied between 0.0032 and 68.2569 for $\alpha = 0$. Initially, it remains same for the production period of 3 months and increases faster with a small increase of time. Finally its increase rate slows down for longer period of time. The trend is almost the same for the other values of α but the magnitude of I_{mi} is decreased up to $\alpha = 0.4$ and then increased as depicted in the figure. In Figure 7, the value of I_{mi} changes from 0.0007 to 10.3108 for $\alpha = 0.2$. The magnitudes of I_{mi} are much less than that acquired earlier. This indicates the existence of fluid memory in nature because the consideration of α affects the resulting values of the memory part. However, the figure

indicates a strong dependency of the value of I_{mi} to the variation of α that affected the stress-strain relationship. At the beginning of the production, the memory part decreases to a value of 0.0006 and remains constant for the period of 3 months. After this, it starts to increase faster with the increase of time. The increasing rate of the memory part slows down after 19 months of production which continues until the end of the reservoir production life.

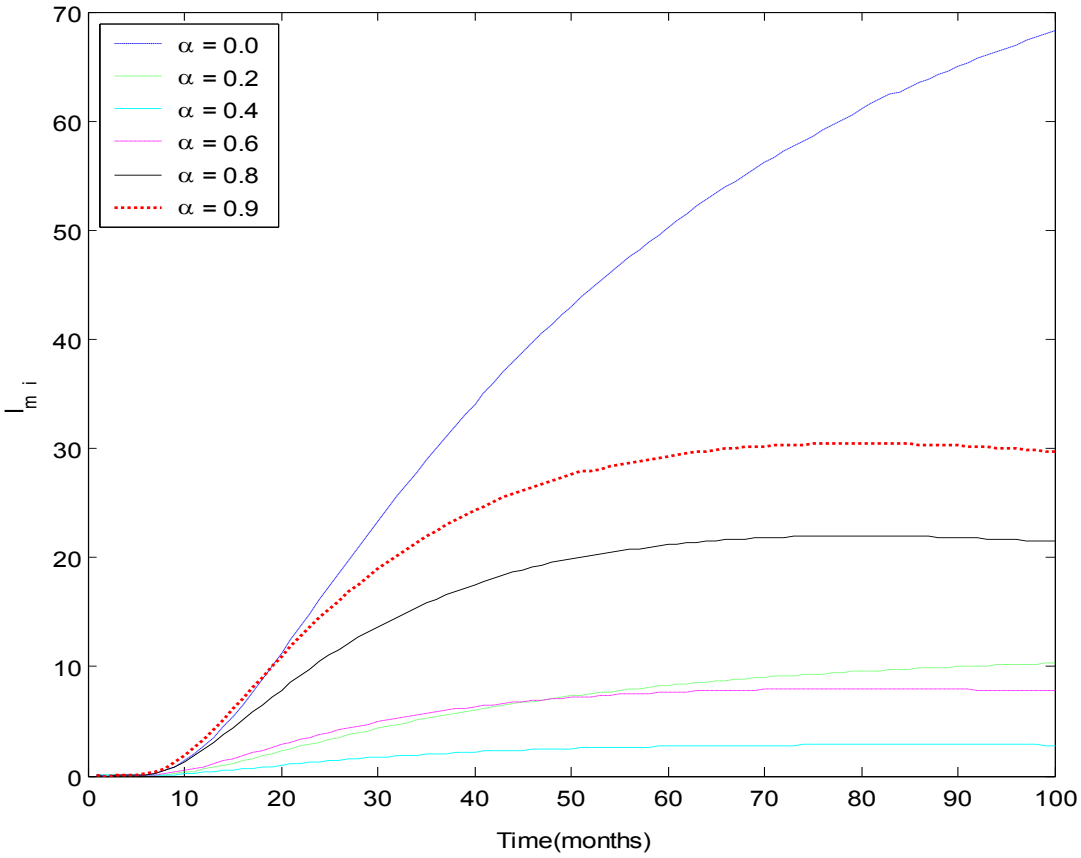

Figure 7 change of memory part over time as a function of different α values at a distance of 1500 m from the wellbore

Figure 7 shows also that, for $\alpha = 0.4$, I_{mi} changes from 0.0002 to 2.8260 which are lower than the latter values. As production begins, I_{mi} decreases up to 0.0001 after 2 months of production and increases gradually up to 0.0651 for a period of 8 months. After this time, it increases faster with the increase of production time. This trend remains up to 2.8555 for the period of 84 months and remains same up to 86 months and then starts to decrease with time. For $\alpha = 0.6$, I_{mi} changes from 0.0002 to 7.7677 which are greater than those corresponding to $\alpha = 0.4$. The memory part decreases very fast up to 0 for a small production period of 2 months whereas it remains same in the previous two α values. These changes show the

chaotic and unpredictable fluid flow within the reservoir due to its inherent fluid memory. After this point, it increases very fast with increase of production time up to a level of 6.9868 for 47 months and then the increasing trend slows down for 7.9595 at 79 months. This trend starts to decrease with time beyond this production period. In addition, the magnitude of I_{mi} varies between 0.0006 and 21.4586, which is plotted for $\alpha = 0.8$. These values are greater than those obtained for $\alpha = 0.6$. The memory part decreases very fast up to 0 for a small production period of 2 months. After this point, it increases faster with increase of production time up to a level of 20.9505 for 58 months and then the increasing trend slows down for 21.9887 at 79 months. This trend starts to decrease with time beyond this production time. For $\alpha = 0.9$, I_{mi} varies between 0.0009 and 29.7228 (see Figure 7). The magnitude of I_{mi} is greater than that of the previous α. This case displays a decreasing trend, which is similar to that obtained for $\alpha = 0.8$. However, this trend increases faster with increase of production time up to a level of 29.9437 for 66 months and then the increasing trend slows down for 30.4571 at 80 months.

Figure 8 shows the change of I_{mi} for different α values during a production period of 100 months at a distance of 3000 m from the wellbore. For $\alpha = 0$, I_{mi} changes from 1.9049 to 107.2981. Initially, it increases gradually up to 3.5120 for the production period of 4 months and then increases rapidly with a small increase of time. It gradually tends to reach its steady state in the long term. For $\alpha = 0.2$, I_{mi} varies from 0.4309 to 15.5123. This is much less than that encountered in the previous case but much greater than the one shown in Figure 7. This indicates that memory effects increase with the increase of time and distance. I_{mi} increases gradually from the beginning of production to 4 months and then increases rapidly with a small increase of time. It tries to reach its steady state in the long term. For $\alpha = 0.4$, I_{mi} changes from 0.1022 to 3.4149. This magnitude is less than the previous one obtained for $\alpha = 0.2$, but much greater than the one in the case of Figure 7. I_{mi} decreases very fast up to 0.0663 after 2 months of production and increases also very fast with increase of product on time. This trend remains the same up to 3.6038 for the period of 63 months and then starts to decrease with time. For $\alpha = 0.6$, I_{mi} variation of 0.1276 to 8.5740 is greater than those changes observed for $\alpha = 0.4$. This is due to the chaotic and unpredictable behavior of fluid which is explained by fluid memory. Here, I_{mi} decreases very fast to 0 for a small production period of 2 months. After this point, it increases very fast with increase of time of production. This trend remains the same up to 9.4141 for the period of 51 months and then starts to decrease with time. For $\alpha = 0.8$, I_{mi} varies from 0.3488 to 23.6813. These values are greater than those obtained for $\alpha = 0.6$. I_{mi} decreases very fast up to 0 for 2 months and increases very fast with increase of time of production. This trend remains the same up to 26.0396 for the period of 50 months and then starts to decrease with production time. For $\alpha = 0.9$. I_{mi} varies from 0.4834 to 32.8016 which are greater than those for $\alpha = 0.8$ of Figure 8 and $\alpha = 0.9$ of Figure 7. I_{mi} decreases very fast to 0 for 2 months and increases very fast with increase of production time. This trend remains the same up to 36.0949 for the period of 50 months and then starts to decrease with production time.

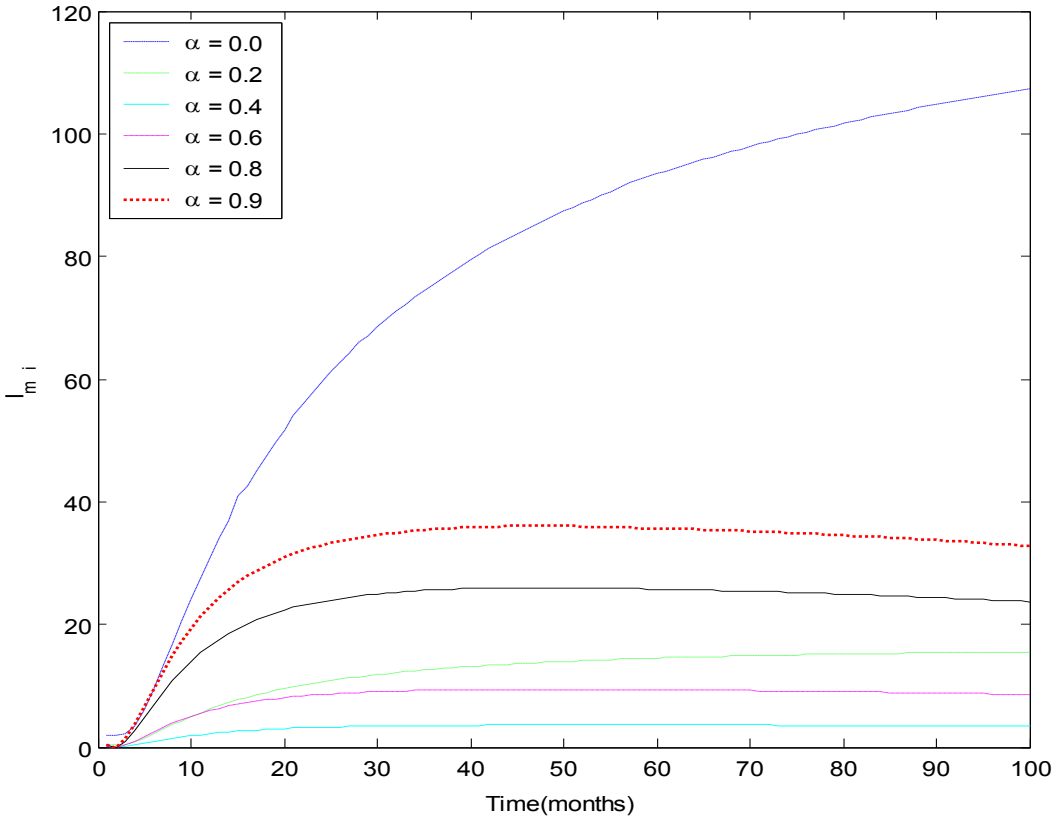

Figure 8 change of memory part over time as a function of different α values at a distance of 3000 m from the wellbore

Figure 9 shows the variation of I_{mi} for different α values for a production duration of 100 months at a distance of 4500 m from the wellbore. For $\alpha = 0$, I_{mi} varies from 65.7528 to 153.5833. Initially, it increases rapidly with a small increase of time and gradually tries to reach steady state with time. For $\alpha = 0.2$, I_{mi} changes from 15.4573 to 20.9319. These values are much less than those given in the previous case, but much greater than those of Figure 8. This indicates that memory effects increase with the increase of distance from the wellbore and shows also a strong influence of fluid memory. I_{mi} increases very fast at the beginning of production. This goes to its peak value of 22.9698 after 13 months of the production and then starts to reduce with time. The decreasing trend expedite towards the end of production life. For $\alpha = 0.4$, I_{mi} varies from 4.2367 to 3.1239 which are much less than those obtained for $\alpha = 0.2$. Here I_{mi} value is much higher at the beginning of production and less at the end period of production comparing with the case of 3000 m shown in Figure 8. However, I_{mi} increases very fast up to 5.0823 after 4 months of production and goes down also very fast with increase of production time. For $\alpha = 0.6$, I_{mi} ranges from 7.5237 to

4.9563 which are greater than those acquired for $\alpha = 0.4$. This behavior is similar to the previous one of Figure 8. Here, I_{mi} increases very fast up to 9.2729 after 4 months of production and goes down also very fast with increase of time of production. Figure 9 shows also the plot for $\alpha = 0.8$ where I_{mi} varies from 20.7022 to 13.6660. The magnitudes are greater than the previous $\alpha = 0.6$. I_{mi} increases very fast up to 26.1875 for a shorter period of production time, 3 months, and after that time, it goes down gradually with increase of time of production. In the same figure, the variation of I_{mi} is shown for $\alpha = 0.9$ which varies from 28.6935 to 18.9291. The trend and magnitudes of I_{mi} are greater than those of $\alpha = 0.8$ which increases very fast up to 36.2959.

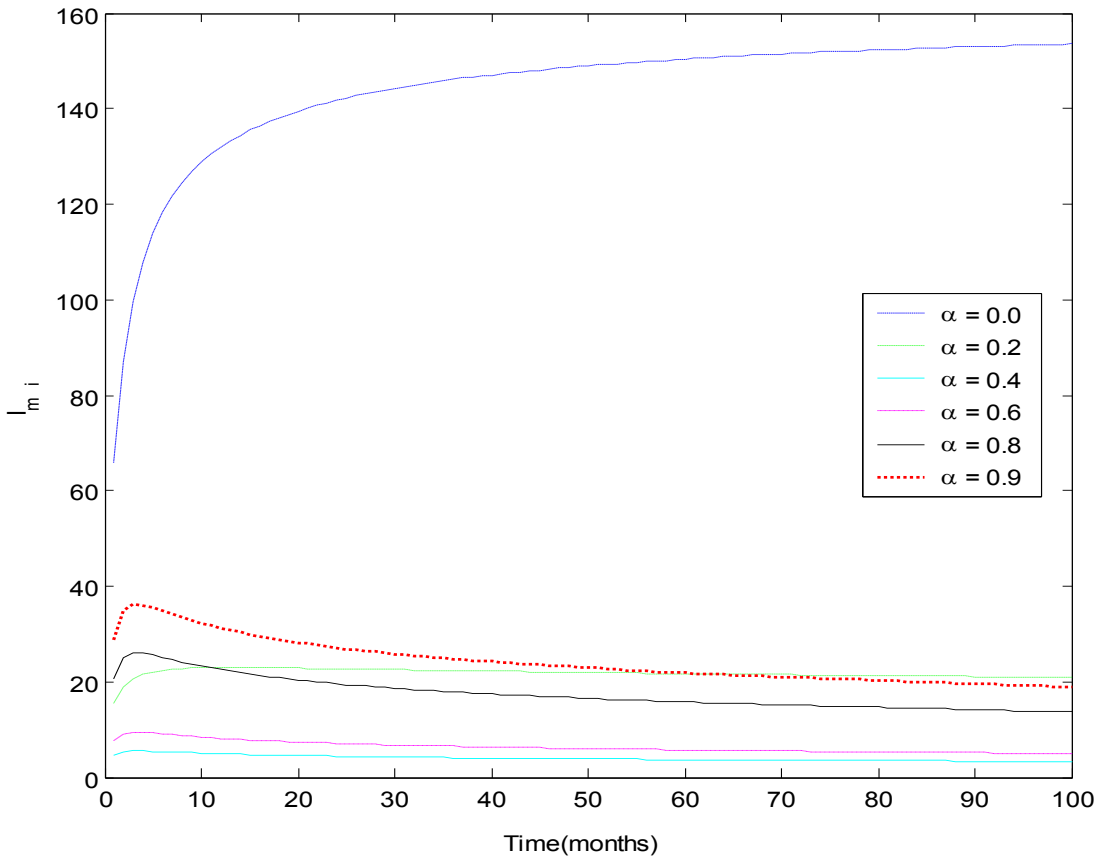

Figure 9 change of memory part over time as a function of different α values at a distance of 4500 m from the wellbore

At different reservoir production life

As indicated earlier in this study, memory is a property of a fluid which represents the history of a fluid. So, time is the most important parameter here. Moreover, I_{mi} is a function of time whereas the pressure gradient changes over time in the x direction ($\partial^2 p / \partial t\, \partial x$) is also a function of time. Therefore, the reservoir life is considered to analyze memory of fluid. The convolution integral part, $I_{ci} = \left\{ \int_0^t (t-\xi)^{-\alpha} \left[\partial^2 p / \partial \xi\, \partial x \right] d\xi \right\}^{0.5}$ i.e. only the numerator is considered in computation because there is no time dependency in the denominator. In this study, reservoir production life is considered as 10, 50 and 100 months.

Table 1 shows the different data of the convolution integral part at different reservoir distance from the wellbore for the reservoir life of 10 months. The data shows that when distance from the wellbore increases, the variation of I_{ci} increases for a particular value of α. I_{ci} also increases with the increases of α. This indicates that memory effect is more dominant as the distance increase from the wellbore. Figure 10 shows the variation of I_{ci} as a function of α for all the data showed in Table 1. The shape and pattern except the magnitude of I_{ci} of the figures are identical for different distances. The common trend of all figures are initially decreasing and then after approximately $\alpha = 0.5$, I_{ci} starts to increase with the increase of α value.

Table 1 Numerical values of I_{ci} for different α values in different distances for a reservoir life of 10 months

Value of α	I_{ci} for 10 months		
	x = 1500 m	x = 3000 m	x = 4500 m
0.0	1.3713	24.1142	128.7294
0.2	0.3369	5.3832	24.7316
0.4	0.1987	2.2587	5.7501
0.6	0.7158	7.5266	12.5635
0.8	2.8485	29.9444	49.8758
0.9	5.6840	59.75116	99.5226

A Novel Memory Based Stress-Strain Model for Reservoir Characterization

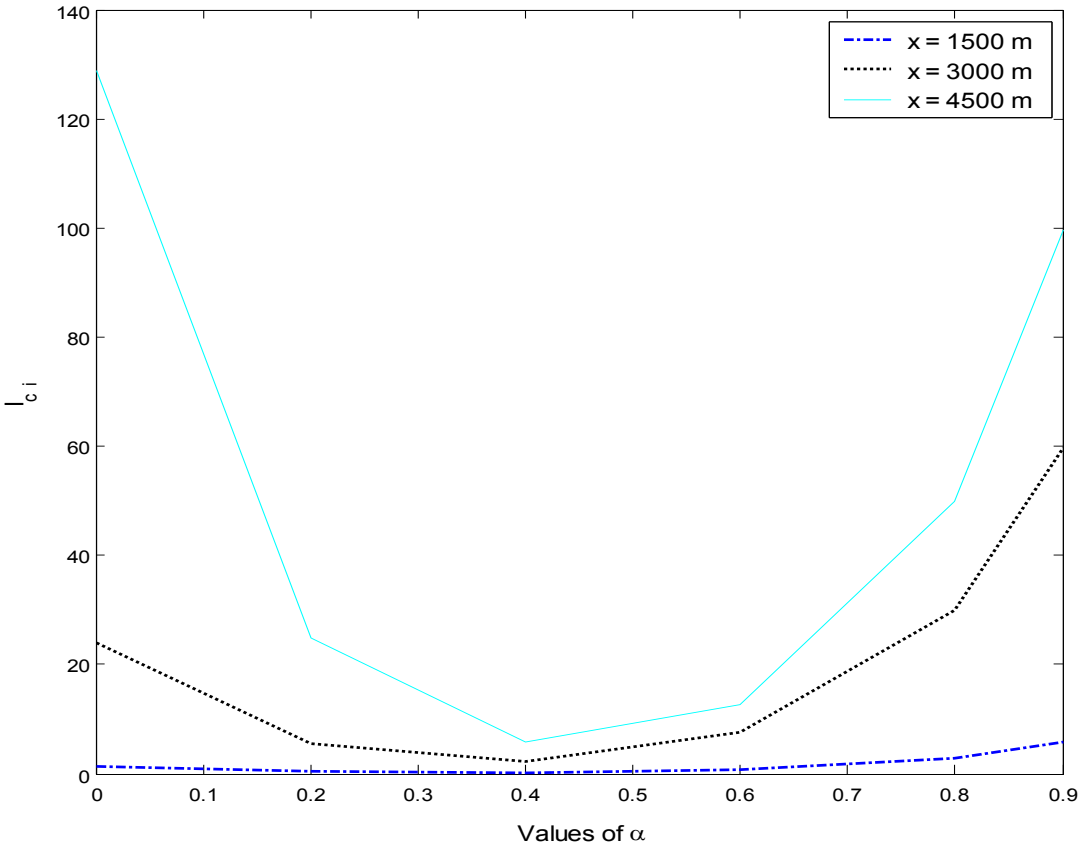

Figure 10 change of memory part over α values for the reservoir life of 10 months at different distance from the wellbore

Table 2 shows the different data of I_{ci} at different reservoir distance from the wellbore for the reservoir life of 50 months. The data shows that when distance from the wellbore increases, the variation of I_{ci} increases for a particular value of α up to $\alpha = 0.2$ and beyond this, it decreases with α . This indicates a chaotic behavior of α values. Figure 11 shows the variation of I_{ci} as a function of α for all the data showed in Table 2. This is same as Figure 10 except the magnitude of I_{ci}.

Table 2 Numerical values of I_{ci} for different α values in different distances for a reservoir life of 50 months

Value of α	I_{ci} for 50 months		
	x = 1500 m	x = 3000 m	x = 4500 m
0.0	42.9970	87.3485	148.9504
0.2	7.9002	15.0594	23.6703
0.4	3.0771	4.4089	4.3923
0.6	10.7237	14.0209	8.9366
0.8	42.6821	55.7932	35.4989
0.9	85.1688	111.3310	70.8352

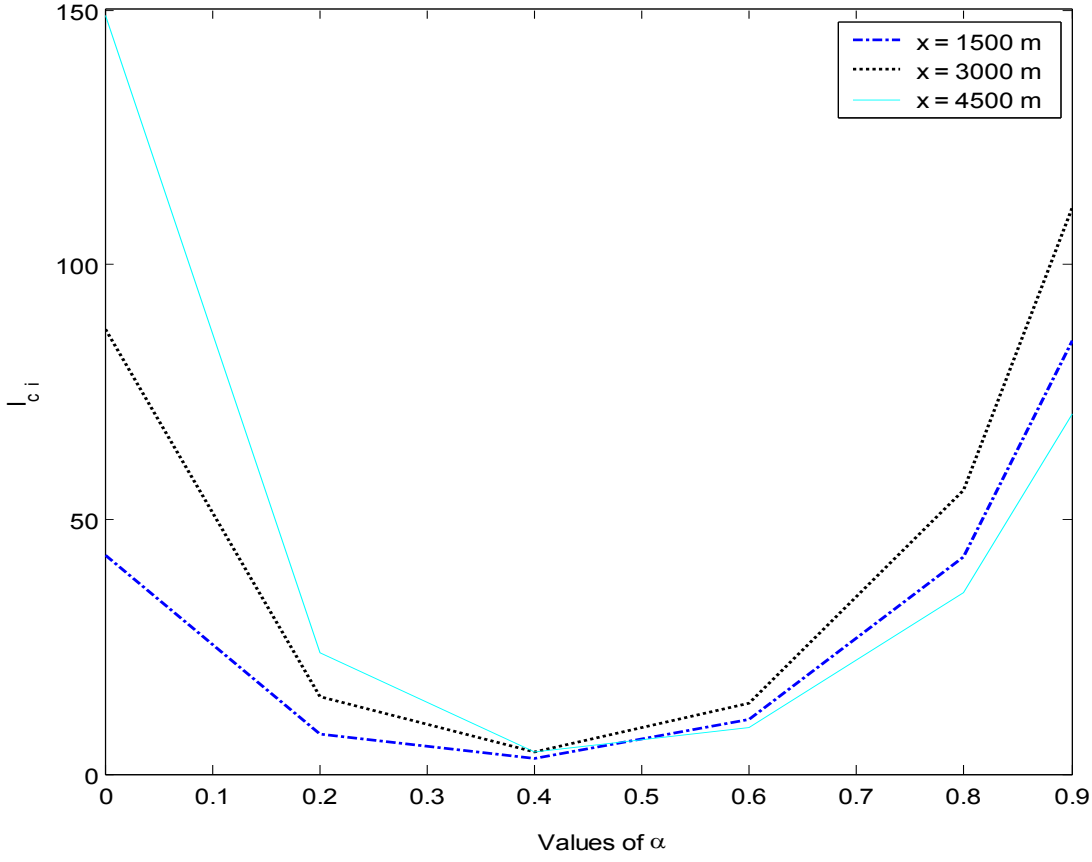

Figure 11 change of memory part over α values for the reservoir life of 50 months at different distance from the wellbore

Table 3 shows the different data of I_{ci} at different reservoir distance from the wellbore for the reservoir life of 100 months. The data shows that when distance from the wellbore increases, the variation of I_{ci} increases for a particular value of α up to $\alpha = 0.2$ and beyond this, it decreases with α. Figure 12 shows the variation of I_{ci} as a function of α for all the data showed in Table 3. This is same as Figure 11 except the magnitude of I_{ci}.

Table 3 Numerical values of I_{ci} for different α values in different distances for a reservoir life of 100 months

Value of α	I_{ci} for 100 months		
	x = 1500 m	x = 3000 m	x = 4500 m
0.0	68.2569	107.2981	153.5833
0.2	11.1253	16.7377	22.5854
0.4	3.4487	4.1673	3.8121
0.6	11.5688	12.7697	7.3816
0.8	45.9777	50.7402	29.2812
0.9	91.6770	101.1732	58.385

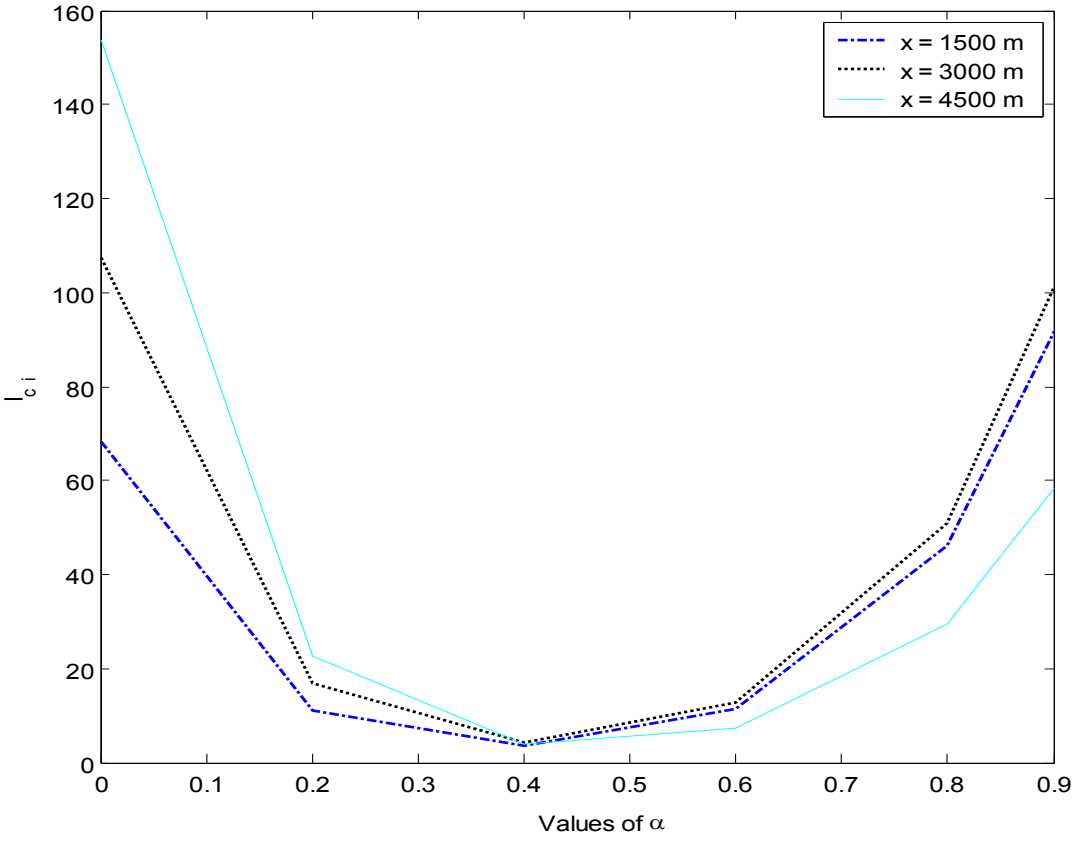

Figure 12 change of memory part over α values for the reservoir life of 100 months at different distance from the wellbore

CONCLUSIONS

A comprehensive model is introduced for stress-strain rate involving the fluid memory effect. It takes into account the influence of temperature, pressure, and surface tension variations. The effect of temperature on viscosity is applied by using the Arrhenius model. This model expresses the variation of temperature with an exponential function. The pressure variation is applied using the Darcy's law. This law is an experimental relation that is extensively used in the fluid flow in porous media. The effect of surface tension is included through the Marangoni number. This model gives the surface tension gradients along a gas–oil interface which provokes strong convective activity, called Marangoni effect. The fluid memory is incorporated with application of α variation.

The memory effect causes a nonlinear relation between the stress and strain rate. The part of the stress-strain formulation related to the memory is taken into account and we obtain the variation of it with time and distance for $0 \le \alpha < 1$. The memory part that is denoted by I_{mi} in the paper has a mild variation for a time duration of 100 months near the wellbore. The variation of I_{mi} is increased as the distance increase from the wellbore. It contained a peak value and then the value of I_{mi} increased mildly if the value of α is less than 0.5. The variation of I_{mi} is increased with increasing the value of α after that value of α. The distance from the wellbore also affects the fluid memory part in the developed model. The memory effects increase with the increase of distance from the wellbore at the beginning of production or for a shorter reservoir life. When the life of the reservoir increases, the memory effects increase for lower values of α whereas they decrease for higher values of α. The variation of distance and time defines a chaotic behavior with increasing and decreasing trends due to α variation in I_{mi} and I_{CS} magnitudes, which gives a strong indication of memory effect. This paper reveals that the memory mechanism helps in interpreting the reservoir phenomenology in addition to other parameters such as matrix heterogeneity, anisotropy, and inelasticity.

NOMENCLATURE

A_{yz} = Cross sectional area of rock perpendicular to the flow of flowing fluid, m^2

c = total compressibility of the system, $1/pa$

E = activation energy for viscous flow, *KJ/mol*

h_f = height in temperature gradient (height between the two points along the *y*-direction) or in other words, thin film thickness of flowing fluid, *m*

k = initial reservoir permeability, m^2

K = operational parameter

L = distance between production well and outer boundary along x direction, *m*

M_a = marangoni number

p = Pressure of the system, N/m^2

p_i = initial pressure of the system, N/m^2

q_x = fluid mass flow rate per unit area in *x*-direction, $kg/m^2 - s$

q_i = Au = initial volume production rate, m^3/s

R = universal gas constant, $kJ/mole - k$

T = temperature, °K

t = time, *s*

ξ = a dummy variable for time i.e. real part in the plane of the integral

u = filtration velocity in *x* direction, m/s

u_x = fluid velocity in porous media in the direction of *x* axis, *m/s*

y = distance from the boundary plan, *m*

ϕ = porosity of fluid media, m^3/m^3

σ = surface tension, *N/m*

α = fractional order of differentiation, dimensionless

α_D = thermal diffusivity, m^2/s

μ = fluid dynamic viscosity, *Pa-s*

μ_0 = fluid dynamic viscosity at reference temperature T_0, *Pa-s*

μ_T = fluid dynamic viscosity at a temperature *T*, *Pa-s*

τ = shear stress, *Pa*

τ_T = shear stress at temperature *T*, *Pa*

$\frac{du_x}{dy}$ = Velocity gradient along y-direction, $1/s$

ΔT $= T_T - T_0 = T_D - T_A$ = temperature difference (Figure 1), °K

ρ_o = density of the fluid at reference temperature T_0, kg/m^3

$p(x, t)$ = fluid pressure, *pa*

η = ratio of the pseudopermeability of the medium with memory to fluid viscosity, $m^3 s^{1+\alpha}/kg$

$\left|\frac{\partial \sigma}{\partial T}\right|$ = the derivative of surface tension σ with temperature and can be positive or negative depending on the substance, *N/m-K*

ACKNOWLEDGEMENT

The authors would like to thank the Atlantic Canada Opportunities Agency (ACOA) for funding this project under the Atlantic Innovation Fund (AIF).

REFERENCES

Abel, M. S., Khan, S. K., Prasad, K.V. 2002. Study of visco-elastic fluid flow and heat transfer over a stretching sheet with variable viscosity. International Journal of Non-Linear Mechanics, 37: 81-88

Avramov, I. 2005. Viscosity in disordered media. Journal of Non-Crystalline Solids, 351: 3163–3173

Brenner, H. 2005. Navier–Stokes revisited. Physica A 349, 60–132

Broszeit, J. 1997. Finite-element simulation of circulating steady flow for fluids of the memory-integral type: flow in a single-screw extruder. Journal of Non-Newtonian Fluid Mechanics, May, Vol –70, Issues – 1-2, 35-58.

Caputo, M. 1999. Diffusion of fluids in porous media with memory. Geothermics, 23, 113-130.

Ciarletta, M. and Scarpetta, E. (1989). Minimum Problems in the Dynamics of Viscous Fluids with Memory. International Journal of Engineering Science, Vol – 27, No – 12, 1563-1567.

D'Aubeterre, A., Silva, R. Da, and Aguilera, M.E., 2005. Experimental Study on Marangoni Effect Induced by Heat and Mass Transfer. International Communications in Heat and Mass Transfer 32: 677-684.

Das, K.S., and Bhattacharjee, J.K. 1999. Marangoni Attractors. Physica A, 270: 173-181.

Eringen, A. C. 1991. Memory Dependent Orientable Nonlocal Micropolar Fluids. International Journal of Engineering Science, Vol – 29, No – 12, 1515-1529.

Gan, Q., Xue, M., and Rooney, D. 2006. A study of fluid properties and microfiltration characteristics of room temperature ionic liquids $[C_{10\text{-}min}][NT_{f2}]$ and $N_{8881}[NT_{f2}]$ and their polar solvent mixtures. Separation and Purification Technology, in press

Haferl, S., and Poulikakos, D. 2003. Experimental Investigation of the transient impact fluid dynamics and solidification of a molten micro droplet pile-up. International Journal of Heat and Mass Transfer, 46: 535-550.

Haminiuk, C.W.I., Sierakowski, M.R., Vidal, J.R.M.B., and Masson, M.L. 2006. Influence of temperature on the rheological behavior of whole araca´ pulp (Psidium cattleianum sabine). LWT, 39: 426–430

Hossain, M. E., Mousavizadegan, S. H. and Islam, M. R. 2006a. Rock and Fluid Temperature Changes during Thermal Operations in EOR Processes. Journal Nature Science and Sustainable Technology, in press

Hossain, M.E. and Islam, M.R. 2006b. Fluid properties with memory – A critical Review and some additions. Proceeding of 36th Int. Conf. Comp. Ind. Eng., June 20-23, Taipei, Taiwan, Paper Number: CIE – 00778.

Hu, X., and Cushman, H., 1994. Non equilibrium statistical mechanical derivation of a nonlocal Darcy's law for unsaturated/saturated flow. Stochastic Hydrology and Hydraulics, 8, 109-116.

James, M.L, Smith, G.M., and Wolford, J.C. 1993. Applied Numerical Methods for Digital Computation. HarperCollins College Publishers, Fourth edition, New York, NY 10022, USA, p. 614.

Jossi, J.A., Stiel, L.I., and Thodos, G., 1962. The viscosity of pure substance in the dense gaseous and liquid phases. A.I.Ch.E. Journal, 8, 59.

Kozak, R., Saghir, M.Z., and viviani, A. 2004. Marangoni Convection in a liquid layer overlying a Porous Layer with Evaporation at the free Surface. Acta Astronautica, 55: 189-197

Li, H.Z., Frank, X., Funfschilling, D., Mouline, Y. 2001. Towards the Understanding of Bubble interactions and Coalescence in non-Newtonian Fluids: a cognitive approach. Chemical Engineering Science, 56, 6419-6425.

Lyford, P., Pratt, H., Greiser, F., Shallcross, D. 1998a. The Marangoni Effect and Enhanced Oil Recovery Part 1. Porous Media Studies. Can. J. Chem. Eng., 76, April, 167-174.

Lyford, P., Pratt, H., Greiser, F., Shallcross, D. 1998b. The Marangoni Effect and Enhanced Oil Recovery Part 2. Interfacial Tension and Drop Instability. Can. J. Chem. Eng., 76, April, 175-182.

Nibbi, R. 1994. Some properties for Viscous Fluids with Memory. International Journal of Engineering Science, Vol – 32, No – 6, 1029-1036.

Recondo, M.P., Elizalde, B.E., and Buera, M.P. 2005. Modeling temperature dependence of honey viscosity and of related supersaturated model carbohydrate systems. Journal of Food Engineering, in press

Bragard, J. and Velarde, M. 1998. Benard –Marangoni convection: Planforms and related theoretical predictions. J of Fluid Mechanics, Vol – 368, August 10, 165-195.

Zuritz, C.A., Puntes, E. M., Mathey, H.H., Pe´rez, E.H., Gasco´n, A., Rubio, L.A., Carullo, C.A., Chernikoff, R.E., and Cabez, M.S. 2005. Density, viscosity and coefficient of thermal expansion of clear grape juice at different soluble solid concentrations and temperatures. Journal of Food Engineering, 71: 143–149.